

***Citation for the published version:***

Yanting Xie, Y., Zheng, J., Wang, Y., Wang, J., Yang, Y., Liu, X., & Chen, Y. (2018). One-step hydrothermal synthesis of fluorescence carbon quantum dots with high product yield and quantum yield. *Nanotechnology*. DOI: 10.1088/1361-6528/aaf3fb

***Document Version:*** Accepted Version © 2018 IOP Publishing Ltd.

***Link to the final published version available at the publisher:***

<https://doi.org/10.1088/1361-6528/aaf3fb>

***General rights***

Copyright© and Moral Rights for the publications made accessible on this site are retained by the individual authors and/or other copyright owners.

Please check the manuscript for details of any other licences that may have been applied and it is a condition of accessing publications that users recognise and abide by the legal requirements associated with these rights. You may not engage in further distribution of the material for any profitmaking activities or any commercial gain. You may freely distribute both the url (<http://uhra.herts.ac.uk/>) and the content of this paper for research or private study, educational, or not-for-profit purposes without prior permission or charge.

***Take down policy***

If you believe that this document breaches copyright please contact us providing details, any such items will be temporarily removed from the repository pending investigation.

***Enquiries***

Please contact University of Hertfordshire Research & Scholarly Communications for any enquiries at [rsc@herts.ac.uk](mailto:rsc@herts.ac.uk)

# One-step hydrothermal synthesis of fluorescence carbon quantum dots with high product yield and quantum yield

Yanting Xie<sup>a,b,e</sup>, Jingxia Zheng<sup>a,b,e</sup>, Yaling Wang<sup>a,b</sup>, Junli Wang<sup>a,b</sup>, Yongzhen Yang<sup>\*a,b</sup>, Xuguang Liu<sup>\*a,c</sup> and Yongkang Chen<sup>\*d</sup>

<sup>a</sup>Key Laboratory of Interface Science and Engineering in Advanced Materials, Taiyuan University of Technology, Ministry of Education, Taiyuan 030024, China

<sup>b</sup>Research Center on Advanced Materials Science and Technology, Taiyuan University of Technology, Taiyuan 030024, China

<sup>c</sup>College of Materials Science and Engineering, Taiyuan University of Technology, Taiyuan 030024, China

<sup>d</sup>School of Engineering and Technology, University of Hertfordshire, Hatfield, Hertfordshire AL10 9AB, UK

<sup>e</sup>These authors contributed equally to this work and should be considered co-first authors.

Corresponding author. Tel: +86-0351-6014138. E-mail: [yyztyut@126.com](mailto:yyztyut@126.com) (Yongzhen Yang); [liuxuguang@tyut.edu.cn](mailto:liuxuguang@tyut.edu.cn) (Xuguang Liu); [y.k.chen@herts.ac.uk](mailto:y.k.chen@herts.ac.uk) (Yongkang Chen)

## Abstract

A one-step hydrothermal synthesis of nitrogen and silicon co-doped fluorescence carbon quantum dots (N,Si-CQDs) from citric acid monohydrate and silane coupling agent KH-792 with high product yield (PY) of 52.56% and high quantum yield (QY) of 97.32% was developed. This greatly improves both PY and QY of CQDs and provides a new approach for a large-scale production of high-quality CQDs. Furthermore, N,Si-CQDs were employed as phosphors without dispersants to fabricate white light-emitting diodes (WLEDs) with the color coordinates at (0.29, 0.32). It is suggested that N,Si-CQDs have great potential as promising fluorescent materials to be applied in WLEDs.

Keywords: high product yield, high fluorescence quantum yield, carbon quantum dots, hydrothermal reaction, silane coupling agent

---

## 1. Introduction

Various methods have been explored to synthesize carbon quantum dots (CQDs) [1-5], but the low product yield (PY) and quantum yield (QY) limit a further application of CQDs. PY is determined to a relative amount of CQDs obtained once, and the higher PY stands for a more economical method and the higher efficiency. Currently, most of CQDs were prepared in a small amount each time, and studies on CQDs' PY are relatively scarce. Chen, Hou and Zhu et al. reported that the PY values of CQDs were 41.8%, 56% and 58%, respectively [3-5]. Specifically, Tan et al. [6] chose isophorone diisocyanate (IPDI) as the single carbon source, and the PY value of the nitrogen-doped oil-soluble CQDs prepared by the microwave method was about 83%. However, IPDI is harmful to the environment and against the concept of green chemistry. Therefore, an exploration of a green synthesis method of CQDs with high PY for a large-scale of production is necessary.

In addition, another factor limiting a further application of CQDs is the low QY. And QY is an important index to judge whether CQDs are a good type of fluorescent materials, and also an important evidence to consider a practical application of CQDs. Therefore, QY must be taken into account when improving the PY of CQDs. Over recent years, more and more investigations about exploring PY and QY of CQDs have been reported. Hou, Zhu, Dang and Wu et al. investigated the PY and QY of CQDs, respectively [4,5,7,8]. However, their QY values did not exceed 90%. Subsequently, Liu et al. [9] have synthesized CQDs with the QY of 94.5%, however, the PY of CQDs have not been studied. This indicates that it is still a challenge to prepare CQDs with high PY and QY simultaneously.

In CQD's synthesis, Singh et al. adopted red pomegranate [10,11], glucose [12], and beetroot aqueous extract [13] to synthesize CQDs. But their QY is 6% and generally low. Citric acid including rich hydroxyl and carboxyl groups is widely used [4,5,14]. Silane coupling agent KH-792 is a kind of nitrogen-containing additives with long-chains, both acting as a nitrogen dopant and a passivating agent. Zhang et al. [15] synthesized CQDs with the QY value of 57.3% with a

---

hydrothermal method using citric acid monohydrate (CA) and KH-792. However, they have not studied the PY of CQDs and the QY of CQDs prepared by them is not high enough.

Therefore, in order to improve CQD's PY on the premise of ensuring high QY, herein, through optimization of synthesis conditions of CQDs, N,Si-CQDs with high PY (52.56%) and high QY (97.32%) were synthesized by a one-step hydrothermal process through the dehydration condensation of CA and KH-792. It is found that this simple green synthesis method of N,Si-CQDs could provide a new way for a large-scale production of N,Si-CQDs. Benefiting from high QY and good film formability, white light-emitting diodes (WLEDs) were also fabricated with these N,Si-CQDs. Results have indicated that N,Si-CQDs could be the new phosphor for WLEDs. A specific synthesis diagram is shown in Figure 1.

## 2. Experimental section

### 2.1 Materials

Citric acid monohydrate and N-( $\beta$ -Aminoethyl)- $\gamma$ -aminopropyl trimethoxysilane (KH-792) were provided from Tianjin Guangfu Chemical Reagent Co., Ltd with their analytical grades. Deionized water was used throughout all experimental processes in this study.

### 2.2 Synthesis of N,Si-CQDs

N,Si-CQDs were synthesized according to the hydrothermal method reported previously [15]. In a specific experimental process, citric acid monohydrate, the silane coupling agent KH-792 and deionized water were added into a Teflonlined stainless-steel autoclave with 100 mL capacity, heated to certain temperature and kept for a period of time. The molar ratio between CA and KH-792 was set at 1:20. After naturally cooling to the ambient temperature, products were collected and filtered through a polyethersulfone membrane with a 0.22  $\mu$ m mesh. The obtained orange-yellow N,Si-CQD solution was further purified by a dialysis bag (cutoff molecular weight: 1000 Da). This N,Si-CQD solution was dialyzed for 3 h each time (the total dialysis duration can be termed as an accumulative dialysis duration, which is defined as each individual dialysis duration multiplied by the number of dialysis times). Finally, the solution was lyophilized to obtain powder for later characterization.

### 2.3 Characterizations

Transmission electron microscopy (TEM) was conducted and high resolution TEM (HRTEM) images of N,Si-CQDs were obtained by a JEOL JEM-2010 microscope. Fourier transform infrared (FTIR) spectra were measured with a Bruker Tensor 27 spectrometer. X-ray photoelectron spectroscopy (XPS) was performed by a Kratos AXIS ULTRA DLD X-ray photoelectron spectrometer with mono X-ray source Al K $\alpha$  excitation (1486.6 eV). Elemental analysis (EA) measurements were acquired with an ELEMENTAR vario EL cube. Ultraviolet-visible (UV-vis) absorption was recorded on a Hitachi U3900 UV-vis spectrophotometer. The excitation and emission spectra of N,Si-CQD solutions were measured with a Horiba Fluoromax-4 luminescence spectrometer using a Xe lamp as an excitation source. Transient Fluorescence & Phosphorescence (FLS 980) was adopted for measuring the fluorescence decay status and further evaluating the fluorescence lifetime of the N,Si-CQDs.

### 2.4 Calculation of quantum yield (QY)

QY of N,Si-CQDs was obtained by a comparative method. Quinine sulfate (QY=54 $\pm$ 0%) in 0.10 M H<sub>2</sub>SO<sub>4</sub> was chosen as the reference to determine the QY value of N,Si-CQDs in aqueous solution at different concentrations. All the absorbance values of the solutions were measured at 360 nm. Absorbance values were kept under 0.1 at the excitation wavelength for minimizing re-absorption effects. The integrated emission intensity was the area under the emission curve from 380 to 700 nm. The linear fitting lines of the integrated emission intensity against the absorbance were plotted. Finally, QY was calculated as follows:

$$Q = Q_{st}(K/K_{st})(\eta/\eta_{st})^2 \quad (1)$$

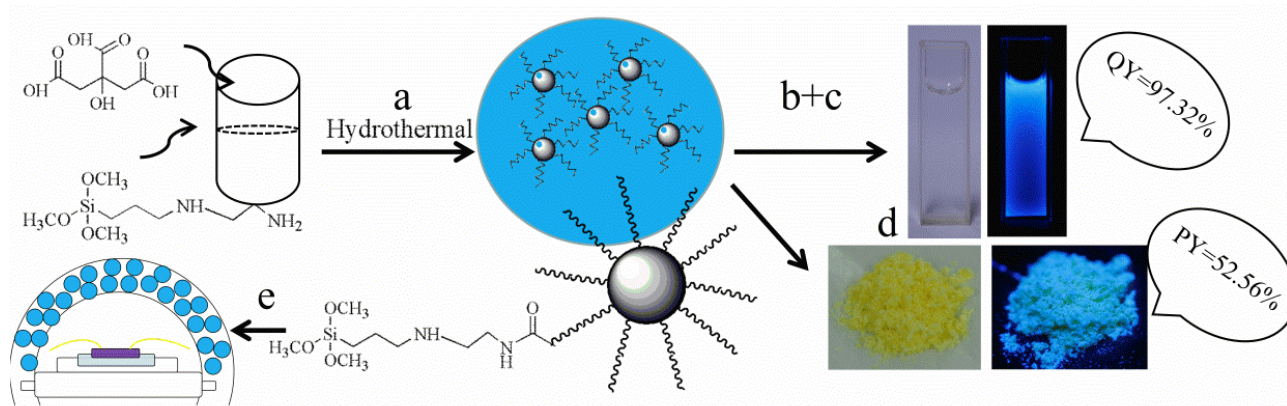


Figure 1. Schematic of N,Si-CQD synthesis

(a. Hydrothermal reacted for a period of time under certain temperature, b. filtered through a polyethersulfone membrane with a 0.22  $\mu\text{m}$  mesh, c. further purified by a dialysis bag (cutoff molecular weight: 1000 Da), d. lyophilized to obtain powder, e. manufacture WLEDs)

Table 1. The PY values of N,Si-CQDs under different reaction conditions (dialysis duration each time was 3 h, the mass of CA was 1.0507 g (0.005 mol), the volume of KH-792 was 21.8 mL (0.1 mol))

Samples	Accumulative dialysis duration/h- Reaction temperature/ $^{\circ}\text{C}$ - Reaction duration/h	PY/%			Mean/%	Standard deviation/%
		1	2	3		
S1	0-200-6	60.85	60.69	60.02	60.52	0.4
S2	3-200-6	53.75	52.82	51.10	52.56	1.1
S3	6-200-6	36.80	37.96	37.28	37.35	0.5
S4	9-200-6	25.37	26.88	26.28	26.18	0.6
S5	3-180-6	46.49	48.48	47.56	47.51	0.8
S6	3-220-6	37.46	36.62	35.88	36.65	0.6
S7	3-200-3	41.15	39.90	37.79	39.61	1.4
S8	3-200-9	29.94	30.58	31.66	30.73	0.7

Note: N,Si-CQDs were repeated synthesized under different reaction conditions for three times, and labeled as 1, 2, 3, respectively

Table 2. The QY values of N,Si-CQDs under different reaction conditions (dialysis duration each time was 3 h, the mass of CA was 1.0507 g (0.005 mol), the volume of KH-792 was 21.8 mL (0.1 mol))

Samples	Accumulative dialysis duration/h- Reaction temperature/ $^{\circ}\text{C}$ - Reaction duration/h	QY/%			Mean/%	Standard deviation/%
		1	2	3		
S1	0-200-6	91.51	90.33	85.98	89.27	2.4
S2	3-200-6	97.94	97.37	96.65	97.32	0.5
S3	6-200-6	97.79	97.13	95.33	96.75	1.0
S4	9-200-6	93.87	93.30	90.15	92.44	1.6
S5	3-180-6	90.74	90.38	88.09	89.73	1.2
S6	3-220-6	91.37	91.10	90.41	90.96	0.4
S7	3-200-3	84.91	84.52	83.82	84.42	0.4
S8	3-200-9	84.86	83.84	83.61	84.10	0.5

Note: N,Si-CQDs were repeated synthesized under different reaction conditions for three times, and labeled as 1, 2, 3, respectively

where Q is QY, K is the slope of the liner fitting line, and  $\eta$  is refractive index of the solvent. In the solutions of this study,  $\eta/\eta_{st}=1$ . The subscript "st" refers to quinine sulfate standard solution.

## 2.5 Determination of product yield (PY)

PY of N,Si-CQDs was obtained by a comparative method. The N,Si-CQDs' solution was transferred to a rotary bottle and placed in an ultra-low temperature refrigerator at  $-80^{\circ}\text{C}$  for 12 h to be frozen. Then, the rotary bottle was attached to the freeze-dried for 48 h to obtain N,Si-CQD solid. The N,Si-CQD solid was ground and placed on a tray balance for weighing. Finally, PY was calculated as follows:

$$\text{PY} = \frac{m_{\text{CQDs}}}{m_{\text{C}} + m_{\text{H}}} \times 100\% \quad (2)$$

where,  $m_{\text{C}}$  refers to the mass of citric acid monohydrate,  $m_{\text{H}}$  refers to the mass of KH-792, and  $m_{\text{CQDs}}$  refers to the mass of the N,Si-CQD solid.

## 2.6 Preparation of WLEDs

The UV LED chip was purchased from Shenzhen Guanghuashi Technology Co., Ltd. A UV chip with the peak wavelength centered at 365 nm was fixed on the bottom of the LED base. Two threads on the LED were applied to connect to the external power supply. Then 10, 15 and 20 mg mL<sup>-1</sup> of N,Si-CQD solution was softly dripped onto the inner wall of the optical lens, respectively, followed by leaving the optical lens in a drying oven at  $80^{\circ}\text{C}$  for 3 h. Finally, the optical lens was solidly fixed on the bottom of the LED chip to realize the fabrication of a WLED.

## 3. Results and discussion

### 3.1 Optical properties of N,Si-CQDs

Accumulative dialysis duration ( $D_{\text{d}}$ ), reaction temperature (T) and reaction duration ( $D_{\text{r}}$ ) are three major factors affecting both PY and QY of N,Si-CQDs, as shown in Tables 1 and 2.

The formation of N,Si-CQDs includes dehydration, polymerization and carbonization [4]. As shown in Figure S1, it can be seen that the color of CA alone and KH-792 alone after hydrothermal treatment is colorless, while the color of the mixed solution of CA and KH-792 is yellow-green. Which confirm that KH-792 is carbonized after mixing with CA in the hydrothermal treatment. First, small fluorescent molecules were generated as CA reacted with KH-792. Subsequently, the small fluorescent molecules were further condensed to form fluorescent polymer chains (FPCs), Next, FPCs were carbonized to form N,Si-CQDs. However, fluorescent small molecules and FPCs might not be completely reacted so that they existed alone or were on the surfaces of N,Si-CQDs. The chemical interactions between fluorescent molecules and N,Si-CQDs can be covalent bonds, supramolecular interactions or physical blending [16]. In summary, as  $D_{\text{d}}$  was increased from 0 to 9 hours (h), N,Si-CQDs' PY value was decreased from 60.52% to 52.56% in the first 3 h, then further decreased to 26.18%, however the QY value was increased from 89.27% to 97.32% in the first 3 h, then decreased again up to 92.44%. As  $D_{\text{d}}$  was gradually increased, the relatively small fluorescent CQDs will be dialyzed out except for the incompletely reacted small molecules, resulting in a gradual decrease of PY values. The QY value mainly depends on the number of FPCs [17]. When  $D_{\text{d}}$  was increased from 3 to 6 h, unreacted small molecules of raw materials could be dialyzed out, therefore the QY value was increased; when  $D_{\text{d}}$  was increased to 9 h, the number of FPCs was also decreased as small CQDs were dialyzed out, so QY decreased. In summary, when  $D_{\text{d}}$  was 3 h, the PY value was 52.56% and QY value reached the highest. Thus,  $D_{\text{d}}$  of 3 h has been chosen for the comprehensive consideration of the purity and QY of N,Si-CQDs.

As shown in Tables 1 and 2, when T was increased from  $180^{\circ}\text{C}$  to  $220^{\circ}\text{C}$ , PY and QY both showed a trend of first increasing and then decreasing. This is consistent with the results reported by the literature [4]. As mentioned early, in the formation of N,Si-CQDs, at first, small fluorescent molecules were generated by an amidation reaction. Then FPCs were formed by condensation, which has an effect on both PY and QY. When T was increased from 180 to  $200^{\circ}\text{C}$ , FPCs were carbonized to form N,Si-CQDs, therefore the PY value was increased from 47.51% to 52.56%. As T was further increased to  $220^{\circ}\text{C}$ , N,Si-CQDs continued to grow and formed large carbon particles and other by-products, resulting in a decrease of the PY to 36.65%. However, QY of N,Si-CQDs mainly depends on the number of FPCs [17]. At  $180\text{--}200^{\circ}\text{C}$ , on one hand, short FPCs were extended to form long FPCs, and on the other hand, parts of the FPCs were consumed for the nucleation of N,Si-CQDs. Since the formation of FPCs is faster than its consumption, the amount of FPCs was gradually increased, and the QY value was increased from 89.73% to 97.32%. At  $200\text{--}220^{\circ}\text{C}$ , the formation rate of FPCs is slower than its consumption rate, relatively speaking, the number of FPCs was gradually decreased, resulting in a QY drop to 90.96%. It is suggested that  $200^{\circ}\text{C}$  should be the optimal reaction temperature.

It can also be seen that when  $D_r$  was increased from 3 h to 9 h, both PY and QY displayed the similar trend of first increase and then decrease. For the PY of N,Si-CQDs, the PY value was increased from 39.61% to 52.56% as  $D_r$  was increased from 3 to 6 h. And the PY value was decreased to 30.73% as  $D_r$  was increased to 9 h. With a further increase of  $D_r$ , N,Si-CQDs continued to grow into large carbon particles and other by-products, resulting in a significant decrease in PY values [4]. For the QY of N,Si-CQDs, when  $D_r$  was increased from 3 to 6 h, the number of FPCs was gradually increased as the reaction proceeded, and the QY was increased from 84.42% to 97.32%. Nucleation of N,Si-CQDs began to occur when the number of FPCs reached a critical saturation point [18]. This is consistent with the results reported by the literature [4]. So when  $D_r$  was increased to 9 h, the QY value was gradually decreased to 84.10% due to more and more FPCs being used for nucleation of N,Si-CQDs [4,17]. Therefore, a period of the 6 h was chosen as the optimal  $D_r$ .

Overall, PY of N,Si-CQDs was decreased gradually with a change of  $D_d$ , but first increased followed by a decrease with a change of either T or  $D_r$ . However, QY of N,Si-CQDs was first increased followed by a decrease with a change of  $D_d$ , T and  $D_r$ . Therefore, it is suggested that the optimal reaction conditions for preparation of N,Si-CQDs are accumulative dialysis duration of 3 h, reaction temperature of 200°C and reaction duration of 6 h.

Table 3. Comparison of product yield (PY) and quantum yield (QY) values of CQDs synthesized using different raw materials and methods

Year	Experimental materials	Synthesis methods	PY/%	Relative QY/%	Absolute QY/%	References
2017	citric acid, ethylenediamine	microwave	-	75.96	-	[19]
2017	1,3,6-trinitropyrene	solvothermal	90	65.93	-	[8]
2017	p-Phenylenediamine (PPDA)	solvothermal	-	-	52.46	[20]
2016	citric acid tris(hydroxymethyl)aminomethane	microwave	88.1	99.3	~99.3	[14]
2016	citric acid, dicyandiamide	solvent-free	56	73.2	-	[4]
2016	hydroquinone, ethylenediamine (EDA)	water at room temperature	-	-	24.6	[21]
2016	polyamide resin ethylenediamine (EDA) silane coupling agent KH570	ultrasound at room temperature	25.7	~28.3	-	[7]
2014	citric acid, Mg(OH) <sub>2</sub> , ethylenediamine (EDA)	hydrothermal	-	83.0	-	[22]
2014	chinese ink	oxidized and cut	78	-	-	[23]
2018	citric acid monohydrate KH-792	hydrothermal	52.56	97.32	-	this article

Table 3 shows a comparison between PY and QY values of CQDs synthesized by adopting different raw materials and methods. As shown in Table 1, the PY value of N,Si-CQDs is 52.56% in the optimal reaction conditions and is much lower value than the QY value of ~90% reported by the literature [8]. In reference [8], Wu et al. produced CQDs with a high yield of 90% by adopting 1,3,6-trinitropyrene as the reaction material. The reasons for high PY of CQDs may lie in three aspects. First, 1,3,6-trinitropyrene has a large benzene ring conjugate structure, and has high carbon-carbon double bond content, which is beneficial to high PY of CQDs [24]. Second, long reaction duration (12 h) favors the carbonization of CQDs which leads to a high PY. Third, there is a difference in purification methods. Their CQDs were purified only by a preliminary

filtration while our N,Si-CQDs were deeply purified by a further dialysis after filtration. In reference [14], the simple purification (centrifugation and filtration) results in a low loss of CQDs, which also makes CQDs show high PY. In reference [23], firstly, high reaction temperature (240°C) and long reaction duration (12 h) facilitate the carbonization and nucleation of CQDs, further contributing to the high PY of CQDs. Secondly, the different purification method (dialysis) also results in a low loss of CQDs. Thus, the CQDs have a higher PY. Table 2 shows that the greatest QY value of N,Si-CQDs is 97.32%, which is slightly lower than the ultra-high QY of 99.3% from Zhang et al. [14]. On the one hand, this super high QY (99.3%) is due to the different nature of the synthesized raw materials; on the other hand, the super high QY is due to a synergistic effect between graphite nitrogen and abundant hydroxyl groups of 1,1,1-tris (hydroxymethyl) ethane [8]. However, the QY value of N,Si-CQDs prepared in this paper was significantly higher than that of most reported CQDs due to the addition of KH-792 which had three effects. First, KH-792, as a surface passivator, introduced a new surface state, which referred to the interaction between the carbogenic core and the organosilane functional groups [25]. Second, KH-792, used as an electron donor, increased the electron cloud density and thereby raised the possibility of electron-hole radiation recombination. Third, KH-792 had a larger steric effect than oxygen-containing functional groups such as -COOH, which promoted the  $\pi$ - $\pi$  interaction between the carbon core and the functional groups [26]. Therefore, the introduction of KH-792 increased the fluorescence emission intensity of N,Si-CQDs, thus leading to the QY improvement.

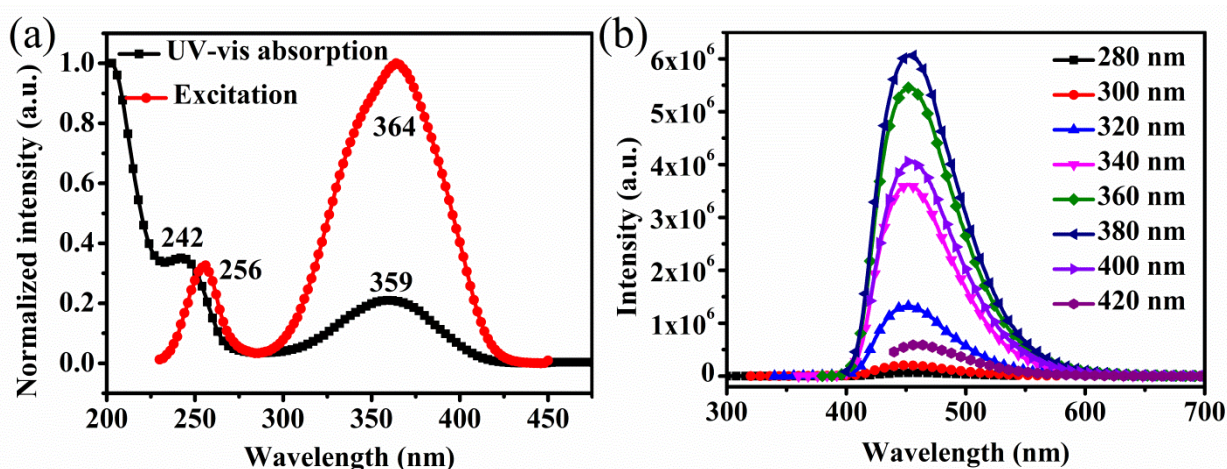


Figure 2. (a) UV-vis absorption and excitation spectra and (b) PL spectra excited at various wavelenghtes of the N,Si-CQD aqueous solution ( $D_d=3$  h,  $T=200^\circ\text{C}$ ,  $D_r=6$  h)

Compared with Zhang et al. [15], the identical reaction conditions are  $D_d$  of 9 h,  $T$  of  $200^\circ\text{C}$  and  $D_r$  for 6 h, and the different reaction conditions is rotational speed of the magnetic rotor used in a dialysis process. The QY value of N,Si-CQDs is 92.44%, which is significantly greater than that (57.3%) reported by Zhang et al. This is mainly because the rotational speed of the magnetic rotor used in a dialysis process is inconsistent ( $10\text{ rpm min}^{-1}$  in this paper,  $30\text{ rpm min}^{-1}$  by Zhang et al.). This indicates that the stirring rate of the magnetic rotor also affects the quality and speed of dialysis. The faster the magnetic stirring speed is, the more loss of small fluorescent molecules is, and the smaller QY values are.

In the optimal conditions ( $D_d=3$  h,  $T=200^\circ\text{C}$ ,  $D_r=6$  h), the UV-vis spectrum shows that N,Si-CQDs present two characteristic absorption peaks at 242 and 359 nm (Figure 2a), which can be assigned to  $\pi$ - $\pi^*$  ( $\text{C}=\text{C}$ ) transition and  $n$ - $\pi^*$  ( $\text{C}=\text{O}$ ) transition, respectively. The excitation spectrum of N,Si-CQDs corresponds to the absorption spectrum. The PL spectra (Figure 2b) indicate that N,Si-CQDs have the property of excitation independence. It is generally agreed that the surface status of CQDs significantly affects PL properties, i.e., surface functional groups primarily respond to trap the excitons under excitation, and the radiative recombination of these surface-trapped excitons leads to the specific PL with corresponding energy. Consequently, CQDs with uniform surface states afford PL with unvaried energies under different excitation wavelengths. Therefore, the excitation-independent property implies uniform surface status of CQDs [20]. It is suggested that the optimal excitation and emission wavelengths are 380 and 453 nm, respectively. Furthermore, the relative QY value of N,Si-CQDs was as great as  $97.32\pm 0.5\%$  (using quinine sulfate as a reference).

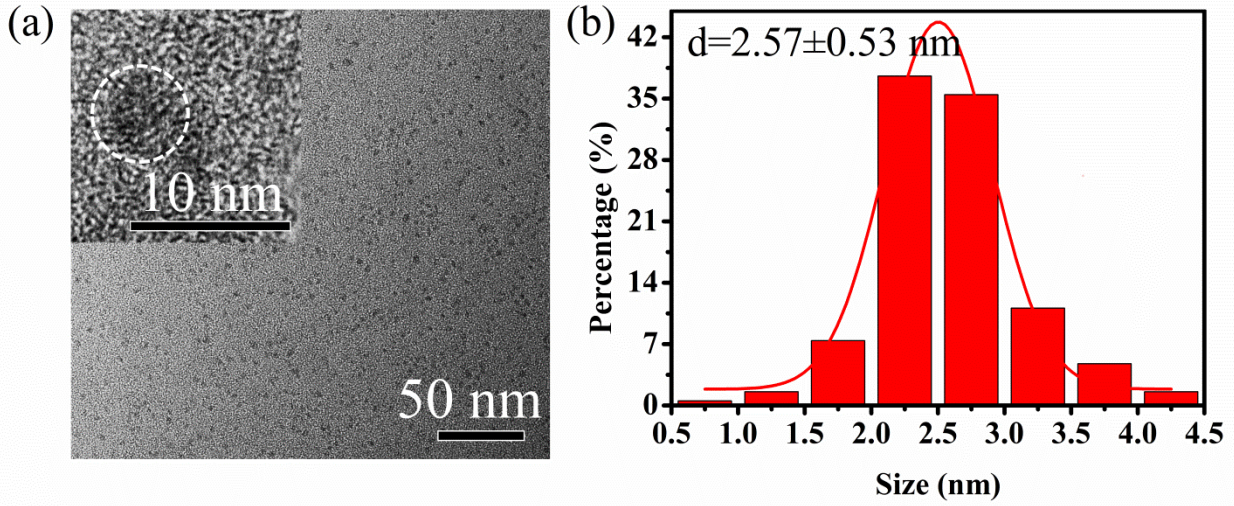


Figure 3. (a) TEM images and (b) the corresponding size distribution histograms of N,Si-CQDs. Inset: HRTEM images of N,Si-CQDs. ( $D_d=3$  h,  $T=200^\circ\text{C}$ ,  $D_r=6$  h)

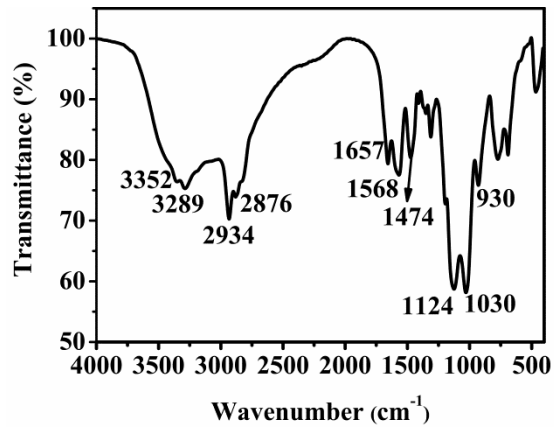


Figure 4. FT-IR spectrum of the N,Si-CQDs ( $D_d=3$  h,  $T=200^\circ\text{C}$ ,  $D_r=6$  h)

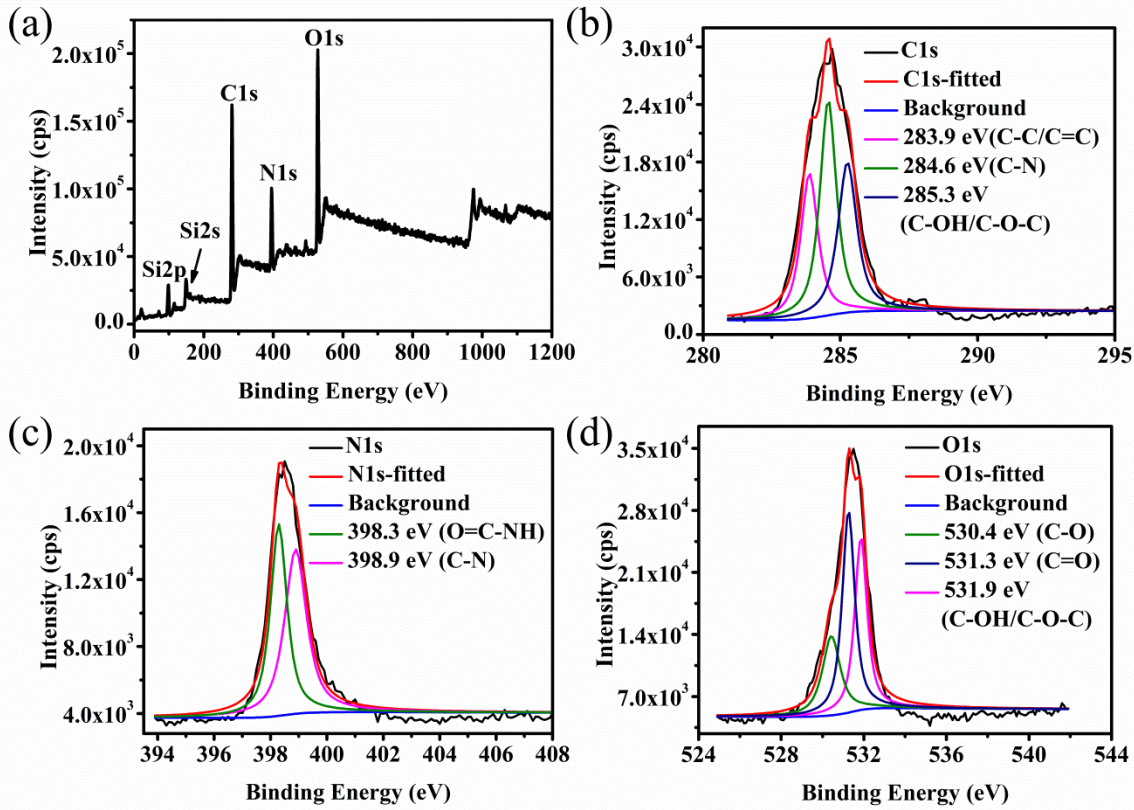


Figure 5. (a) XPS spectra full scan and corresponding high resolution of (b) C1s, (c) N1s, (d) O1s of N,Si-CQDs ( $D_d=3$  h,  $T=200^\circ\text{C}$ ,  $D_r=6$  h)

### 3.2 Morphology and structures of the N,Si-CQDs

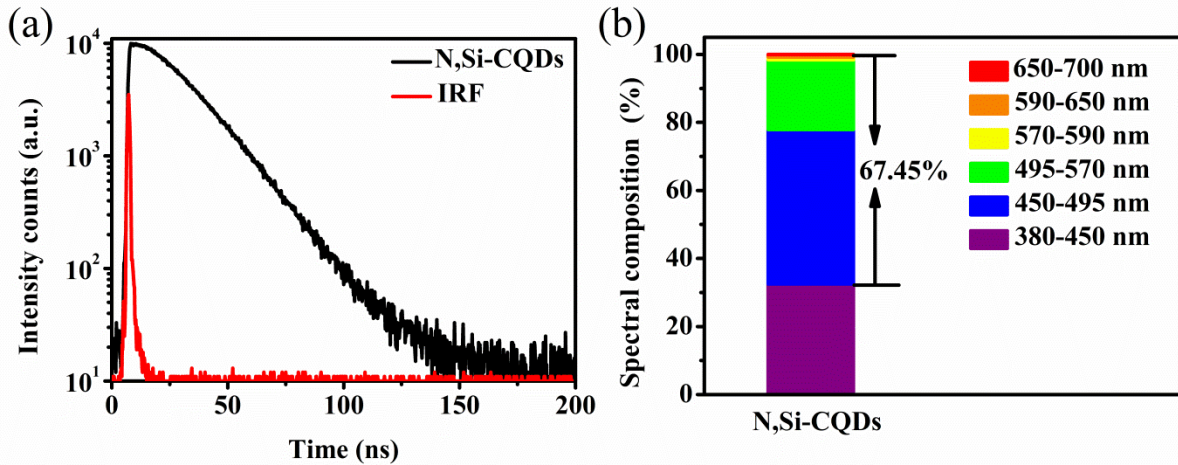


Figure 6. (a) The fluorescence-decay curves and (b) Spectral composition of N,Si-CQDs ( $D_d=3$  h,  $T=200^\circ\text{C}$ ,  $D_r=6$  h), IRF stays for instrumental response function

The TEM (Figure 3) revealed that the N,Si-CQDs are nearly spherical and are well dispersed with an average diameter of 2.57 nm. It can be seen from the inset in Figure 3a that N,Si-CQDs have no obvious lattice stripes but have the amorphous structure.

The FTIR spectrum (Figure 4) demonstrated that the band around  $3367\text{ cm}^{-1}$  corresponds to the vibrations of O-H and N-H. The absorption peak at  $1651\text{ cm}^{-1}$  is attributed to the vibration of -CONH- and the peaks at  $1118$  and  $1033\text{ cm}^{-1}$  are

attributed to the Si-O-Si stretching vibration. These results revealed the occurrence of amidation, confirming that KH-792 was involved in the formation of N,Si-CQDs. The 927  $\text{cm}^{-1}$  is attributed to the out-of-plane deformation vibration of the -OH and O= bands, which has a positive effect on the hydrophilicity of the N,Si-CQDs in aqueous systems.

In the XPS spectrum (Figure 5) of N,Si-CQDs ( $D_d=3$  h,  $T=200^\circ\text{C}$ ,  $D_r=6$  h), as shown in Figure 5a, the strong O1s and C1s peaks demonstrate that N,Si-CQDs mainly consist of carbon and oxygen, whereas the relatively weaker N1s and Si2p peaks demonstrate the formation of new surface states of N,Si-CQDs. As shown in Figure 5b, the C1s spectrum shows three peaks at 283.9, 284.6 and 285.3 eV, which is related to C-C/C=C, C-N and C-OH/C-O-C bonds. As shown in Figure 5c, the N1s spectrum shows two peaks at 398.7 and 399.3 eV, which is related to O=C-NH and C-N bonds. As shown in Figure 5d, the O1s spectrum shows two peaks at 530.4, 531.3 and 531.9 eV, which is related to C-O, C=O and C-OH/C-O-C bonds. Element analysis (EA) of N,Si-CQDs is shown in Table 4. EA was tested to analyze element types and its percentage content. EA results are consistent with the XPS spectrum of N,Si-CQDs. These results demonstrate an involvement of KH-792 in the surface passivation of N,Si-CQDs, which further contributed to the improvement of QY.

To acquire further insight into the photoluminescence, the multidimensional time-correlated single photon counting (TCSPC) method was applied to evaluate the fluorescence lifetime of the N,Si-CQDs. As depicted in Figure 6a, both decay traces were fitted using the biexponential function  $R(t)$  in equation (3):

Table 4. Element analysis of N,Si-CQDs ( $D_d=3$  h,  $T=200^\circ\text{C}$ ,  $D_r=6$  h)

Sample	N	C	H	O	Si
N,Si-CQDs/%	15.29	36.25	7.98	14.71	25.77

Table 5. Biexponential fitting values of N,Si-CQD aqueous solution ( $D_d=3$  h,  $T=200^\circ\text{C}$ ,  $D_r=6$  h)

Sample	$B_1$	$\tau_1$ (ns)	$B_2$	$\tau_2$ (ns)	$\chi^2$	$\langle\tau\rangle$ (ns)
N,Si-CQDs	0.10	9.07	0.90	14.99	1.04	14.62

Table 6. The performance indicators of WLEDs under different test parameters

Concentration/(mg mL <sup>-1</sup> )	Working voltage/V	Color temperature/K	Color coordinates
10	3.0	5650	(0.33,0.38)
	3.1	6027	(0.32,0.37)
	3.2	6546	(0.31,0.36)
	3.3	7321	(0.30,0.34)
	3.4	7960	(0.29,0.33)
	3.5	8269	(0.29,0.32)
	3.6	8225	(0.29,0.32)
15	3.0	5888	(0.32,0.37)
	3.1	6382	(0.31,0.36)
	3.2	7059	(0.30,0.34)
	3.3	8044	(0.29,0.32)
	3.4	8910	(0.28,0.31)
	3.5	9458	(0.28,0.31)
	3.6	9555	(0.28,0.31)
20	3.0	5530	(0.33,0.38)
	3.1	5880	(0.32,0.38)
	3.2	6369	(0.31,0.36)
	3.3	7118	(0.30,0.34)
	3.4	7765	(0.30,0.33)
	3.5	8160	(0.29,0.32)
	3.6	8285	(0.29,0.32)

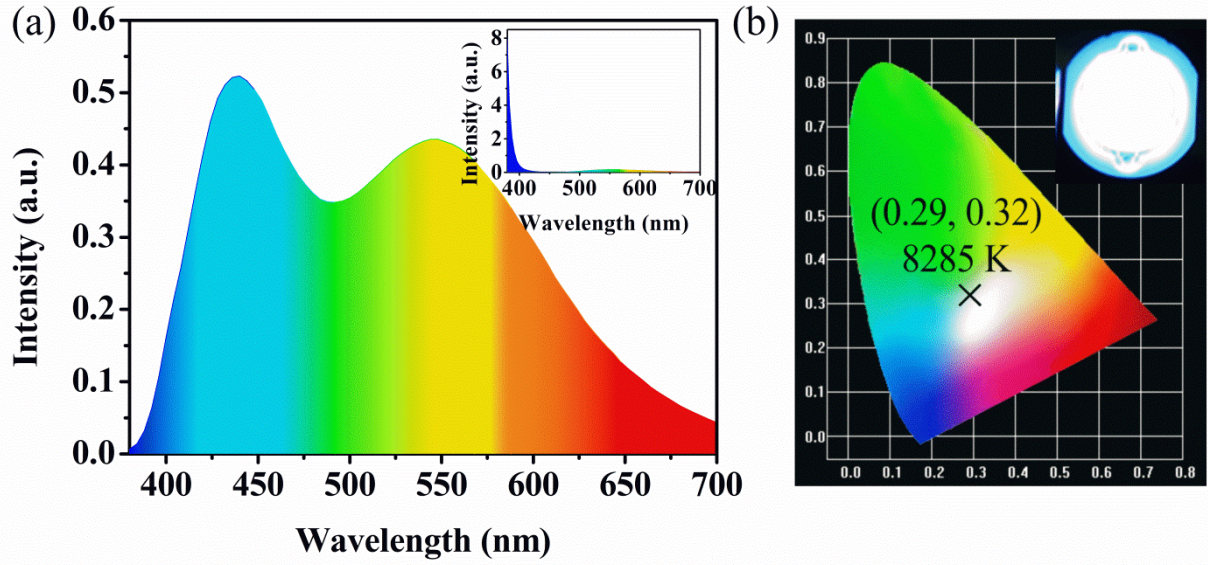


Figure 7. (a) Emission spectrum and (b) CIE chromaticity diagram of WLEDs based on N,Si-CQDs. Inset (a) Emission spectrum of the UV-chip alone and (b) Image of the corresponding WLED at the voltage of 3.6 V ( $D_d=3$  h,  $T=200^\circ\text{C}$ ,  $D_f=6$  h)

$$R(t) = B_1 \exp(-t/\tau_1) + B_2 \exp(-t/\tau_2) \quad (3)$$

where  $B_1$  and  $B_2$  are the pre-exponential factors for the time resolved decay lifetime of  $\tau_1$  and  $\tau_2$ . Then, the average lifetime  $\langle\tau\rangle$  is acquired from equation (4):

$$\tau = \frac{B_1\tau_1^2 + B_2\tau_2^2}{B_1\tau_1 + B_2\tau_2} \quad (4)$$

The fluorescence decay (Figure 6a) and Table 5 showed that N,Si-CQDs ( $D_d=3$  h,  $T=200^\circ\text{C}$ ,  $D_f=6$  h) exhibit biexponential decay and their average lifetime is 14.62 ns. The RGB (blue-to-red) spectral composition (Figure 6b) of N,Si-CQDs is 67.45%. A high RGB spectral proportion is conducive to a promotion in the efficiency of converting UV light into white light, which favours a high color rendering index (CRI) value in the WLEDs. Because the high RGB spectral composition may be attributed to the higher  $\pi$ -electron density on the surfaces of N,Si-CQDs so that it can reduce the energy band gap of  $\pi$ - $\pi^*$  transition in the N,Si-CQD surface state, consequently resulting in a redshift of the emission wavelength, which would make N,Si-CQDs more suitable for a phosphor application in WLEDs [19,27].

### 3.3 WLEDs application of the N,Si-CQDs

WLED devices were obtained benefiting from high QY and unique film-forming property of N,Si-CQDs. Since the concentration of N,Si-CQD solution and the working voltage could affect the properties of WLEDs, they were investigated. As shown in Figure S2, as the concentration of N,Si-CQD solution was increased from 10 to 20  $\text{mg mL}^{-1}$ , the electroluminescent intensity of WLEDs was decreased, but the absorption of WLEDs in the UV region decreased significantly. Therefore, 20  $\text{mg mL}^{-1}$  was chosen as the optimal concentration of N,Si-CQD solution. As shown in Figure S3, with an increase of the working voltage from 3.0 to 3.6 V, the intensity of WLEDs was gradually enhanced. In addition, as shown in Table 6, considering color coordinates and corresponding color temperature (CCT) of WLEDs, 3.6 V was chosen as the optimal working voltage. Under the optimal conditions, the optical performance of WLEDs was characterized. As shown in Figure 7a, it can be seen that the emission spectrum of the device covers the entire visible light region (380–780 nm). As shown in Figure 7b, the color coordinates are (0.29, 0.32), the CRI is 84 and the CCT is 8285 K, which belongs to the cool white gamut. These parameters suggest that N,Si-CQDs have a great potential to be employed in either office or outdoor lighting.

## 4. Conclusions

In short, N,Si-CQDs with high PY (52.56%) and QY (97.32%) have been fabricated by one-step hydrothermal method with CA and KH-792. These synthesized N,Si-CQDs are nearly spherical and with the average particle size of 2.57 nm. The N,Si-CQD solution can emit blue fluorescence under UV light and has an excitation-wavelength independence and good film-forming property. As-prepared WLEDs have the coordinates of (0.29, 0.32), CRI of 84 and CCT of 8285 K. The results reveal that the N,Si-CQDs have a great potential application for office and outdoor lighting. Due to the low cost of raw materials and the simple synthesis approach of N,Si-CQDs, this simple and efficient synthesis method of high-quality CQDs has been developed, which will not only broaden the further application of CQDs, more importantly, but also open up a new approach for a large-scale preparation of CQDs.

## Acknowledgements

This study was supported by National Natural Science Foundation of China (U1710117), Shanxi Provincial Key Innovative Research Team in Science and Technology (2015013002-10, 201605D131045-10) and Shanxi Provincial Key Research and Development Program (201603D111010, 201703D321015-1).

## References

- [1] Sahu S, Behera B, Maiti T K and Mohapatra S 2012 Simple one-step synthesis of highly luminescent carbon dots from orange juice: application as excellent bio-imaging agents *Chem. Commun.* **48** 8835-8837
- [2] Wang J, Peng F, Lu Y, Zhong Y, Wang S, Xu M, Ji X, Su Y, Liao L and He Y 2015 Large-scale green synthesis of fluorescent carbon nanodots and their use in optics applications *Adv. Opt. Mater.* **3** 103-111
- [3] Chen B, et al 2013 Large scale synthesis of photoluminescent carbon nanodots and their application for bioimaging *Nanoscale* **5** 1967-1971
- [4] Hou J, Wang W, Zhou T, Wang B, Li H and Ding L 2016 Synthesis and formation mechanistic investigation of nitrogen-doped carbon dots with high quantum yields and yellowish-green fluorescence *Nanoscale* **8** 11185-11193
- [5] Zhu S, Meng Q, Wang L, Zhang J, Song Y, Han H, Zhang K, Sun H, Wang H and Yang B 2013 Highly photoluminescent carbon dots for multicolor patterning, sensors, and bioimaging *Angew. Chem.* **125** 4045-4049
- [6] Tan J, Zou R, Zhang J, Li W, Zhang L and Yue D 2016 Large-scale synthesis of N-doped carbon quantum dots and their phosphorescence properties in a polyurethane matrix *Nanoscale* **8** 4742-4747
- [7] Dang H, Huang L, Zhang Y, Wang C and Chen S 2016 Large-scale ultrasonic fabrication of white fluorescent carbon dots *Ind. Eng. Chem. Res.* **55** 5335-5341
- [8] Wu M, Zhan J, Geng B, He P, Wu K, Wang L, Xu G, Li Z, Yin L and Pan D 2017 Scalable synthesis of organic-soluble carbon quantum dots: superior optical properties in solvents, solids, and LEDs *Nanoscale* **9** 13195-13202
- [9] Liu H, Li Z, Sun Y, Geng X, Hu Y, Meng H, Ge J and Qu L 2018 Synthesis of luminescent carbon dots with ultrahigh quantum yield and inherent folate receptor-positive cancer cell targetability *Sci. Rep.* **8** 1086
- [10] Singh V and Mishra A K 2015 White light emission from vegetable extracts *Sci. Rep.* **5** 11118
- [11] Singh V and Mishra A K 2016 White light emission from a mixture of pomegranate extract and carbon nanoparticles obtained from the extract *J. Mater. Chem. C* **4** 3131-3137
- [12] Singh V and Mishra A K 2016 Green and cost-effective fluorescent carbon nanoparticles for the selective and sensitive detection of iron (III) ions in aqueous solution: mechanistic insights and cell line imaging studies *Sens. Actuators, B* **227** 467-474
- [13] Singh V et al 2018 Biocompatible fluorescent carbon quantum dots prepared from beetroot extract for in vivo live imaging in *C. elegans* and BALB/c mice *J. Mater. Chem. B* **6** 3366-3371
- [14] Zhang Y, Liu X, Fan Y, Guo X, Zhou L, Lv Y and Lin J 2016 One-step microwave synthesis of N-doped hydroxyl-functionalized carbon dots with ultra-high fluorescence quantum yields *Nanoscale* **8** 15281-15287
- [15] Zhang F, Feng X, Zhang Y, Yan L, Yang Y and Liu X 2016 Photoluminescent carbon quantum dots as a directly film-forming phosphor towards white LEDs *Nanoscale* **8** 8618-8632
- [16] Song Y, Zhu S, Zhang S, Fu Y, Wang L, Zhao X and Yang B 2015 Investigation from chemical structure to photoluminescent mechanism: a type of carbon dots from the pyrolysis of citric acid and an amine *J. Mater. Chem. C* **3** 5976-5984
- [17] Zhang Y, Wang Y, Feng X, Zhang F, Yang Y and Liu X 2016 Effect of reaction temperature on structure and fluorescence properties of nitrogen-doped carbon dots *Appl. Surf. Sci.* **387** 1236-1246
- [18] Sevilla M, Fuertes A B 2009 The production of carbon materials by hydrothermal carbonization of cellulose *Carbon* **47** 2281-2289
- [19] Wang Y, Zheng J, Wang J, Yang Y, Liu X 2017 Rapid microwave-assisted synthesis of highly luminescent nitrogen-doped carbon dots for white light-emitting diodes *Opt. Mater.* **73** 319-329
- [20] Wang J, Zhang F, Wang Y, Yang Y and Liu X 2018 Efficient resistance against solid-state quenching of carbon dots towards white light emitting diodes by physical embedding into silica *Carbon* **126** 426-436
- [21] Chen B, Liu Z, Deng W, Zhan L, Liu M and Huang C 2016 A large-scale synthesis of photoluminescent carbon quantum dots: a self-exothermic reaction driving the formation of the nanocrystalline core at room temperature *Green Chem.* **18** 5127-5132

- 
- [22] Li F, Liu C, Yang J, Wang Z, Liu W and Tian F 2014 Mg/N double doping strategy to fabricate extremely high luminescent carbon dots for bioimaging *RSC Adv.* **4** 3201-3205
- [23] Yang S, Sun J, Li X, Zhou W, Wang Z, He P, Ding G, Xie X, Kang Z and Jiang M 2014 Large-scale fabrication of heavy doped carbon quantum dots with tunable-photoluminescence and sensitive fluorescence detection *J Mater. Chem. A* **2** 8660-8667
- [24] Wang L, Li B, Li L, Xu F, Xu Z, Wei D, Feng Y, Wang Y, Jia D and Zhou Y 2017 Ultrahigh-yield synthesis of N-doped carbon nanodots with down-regulating ROS in zebrafish *J Mater. Chem. B* **5**
- [25] Zou Y, Yan F, Zheng T, Shi D, Sun F, Yang N and Chen L 2015 Wide-bandwidth lasing from C-dot/epoxy nanocomposite Fabry-Perot cavities with ultralow threshold *Talanta* **135** 145-148
- [26] Zhang W, Jin L, Yu S, Zhu H, Pan S, Zhao Y and Yang H 2014 Wide-bandwidth lasing from C-dot/epoxy nanocomposite Fabry-Perot cavities with ultralow threshold *J. Mater. Chem. C* **2** 1525-1531
- [27] Bao L, Liu C, Zhang Z and Pang D 2015 Photoluminescence-tunable carbon nanodots: surface-state energy-gap tuning *Adv. Mater.* **27** 1663-1667